

Radial Flow in Non-Extensive Thermodynamics and Study of Particle Spectra at LHC in the Limit of Small $(q - 1)$

Trambak Bhattacharyya¹, Jean Cleymans², Arvind Khuntia¹, Pooja Pareek¹, and Raghunath Sahoo^{1a}

¹ Discipline of Physics, School of Basic Sciences, Indian Institute of Technology Indore, M.P. 452020, India

² UCT-CERN Research Centre and Department of Physics, University of Cape Town, Rondebosch 7701, South Africa

October 8, 2018

Abstract. We expand the Tsallis distribution in a Taylor series of powers of $(q - 1)$, where q is the Tsallis parameter, assuming q is very close to 1. This helps in studying the degree of deviation of transverse momentum spectra and other thermodynamic quantities from a thermalized Boltzmann distribution. After checking thermodynamic consistency, we provide analytical results for the Tsallis distribution in the presence of collective flow up to the first order of $(q - 1)$. The formulae are compared with the experimental data.

PACS. 1 2.40.Ee - 1 3.75.Cs - 1 3.85.-t - 0 5.70.-a

1 Introduction

It is now a standard practice to use the Tsallis distribution [1] for describing the transverse momentum distributions at high energies. This has been pioneered by the PHENIX and STAR collaborations [2, 3, 4] at the Relativistic Heavy Ion Collider (RHIC) at BNL and by the ALICE, ATLAS and CMS collaborations [5, 6, 7, 8, 9, 10] at the Large Hadron Collider (LHC) at CERN. The Tsallis distribution is successful in explaining the experimental transverse momentum distribution, longitudinal momentum fraction distribution as well as rapidity distribution of hadrons off the e^+e^- as well as $p - p$ collisions [11, 12, 13, 14, 15, 16, 17]. The form of the Tsallis distribution used in this paper has been described in detail previously [18, 19, 20, 21] and has the advantage of being thermodynamically consistent. There is clear evidence for a mild energy dependence of the parameters q and T [20]. Also, initially there were indications that the values obtained for the parameters q and T were consistent with each other for different particle species [17, 19]. Different conclusions have been reached in the literature [22, 23, 24, 25], albeit using slightly different formalisms and approaches, and a more detailed analysis is still outstanding to prove this beyond doubt.

2 Review of the Main Ingredients of the Model

For completeness we recall here the main ingredients.

^a Corresponding Author E-mail: Raghunath.Sahoo@cern.ch

The relevant thermodynamic quantities can be written as integrals over the following distribution function:

$$f = \left[1 + (q - 1) \frac{E - \mu}{T} \right]^{-\frac{1}{q-1}}. \quad (1)$$

It can be shown [19] that the entropy, S , particle number, N , energy density, ϵ , and the pressure, P , are given by,

$$S = -gV \int \frac{d^3p}{(2\pi)^3} [f^q \ln_q f - f], \quad (2)$$

$$N = gV \int \frac{d^3p}{(2\pi)^3} f^q, \quad (3)$$

$$\epsilon = g \int \frac{d^3p}{(2\pi)^3} E f^q, \quad (4)$$

$$P = g \int \frac{d^3p}{(2\pi)^3} \frac{p^2}{3E} f^q. \quad (5)$$

where V is the volume and g is the degeneracy factor.

The function appearing in Eq. (2) is often referred to as q -logarithm and is defined by

$$\ln_q(x) \equiv \frac{x^{1-q} - 1}{1 - q}.$$

The first and second laws of thermodynamics lead to the following two differential relations:

$$d\epsilon = T ds + \mu dn, \quad (6)$$

$$dP = s dT + n d\mu. \quad (7)$$

where, $s = S/V$ and $n = N/V$ are the entropy and particle number densities, respectively.

It is seen that if we use f^q in stead of f to define the thermodynamic variables, the above equations satisfy the thermodynamic consistency conditions which require that the following relations to be satisfied:

$$T = \left. \frac{\partial \epsilon}{\partial s} \right|_n, \quad (8)$$

$$\mu = \left. \frac{\partial \epsilon}{\partial n} \right|_s, \quad (9)$$

$$n = \left. \frac{\partial P}{\partial \mu} \right|_T, \quad (10)$$

$$s = \left. \frac{\partial P}{\partial T} \right|_\mu. \quad (11)$$

Eq. (8), in particular, shows that the variable T appearing in Eq. (1) can indeed be identified as a thermodynamic temperature and is more than just another parameter. It is straightforward to show that these relations are indeed satisfied [19].

Based on the above expressions the particle distribution can be rewritten, using variables appropriate for high-energy physics as

$$\frac{dN}{dp_T dy} = \frac{gV}{(2\pi)^2} p_T m_T \cosh y \left(1 + (q-1) \frac{m_T \cosh y - \mu}{T} \right)^{-\frac{q}{q-1}} \quad (12)$$

It can be shown that at central rapidity, $y = 0$, one can obtain the transverse momentum distribution in terms of the central rapidity density, $dN/dy|_{y=0}$, as the volume dependence can be replaced by a dependence on $dN/dy|_{y=0}$ using

$$\begin{aligned} \frac{dN}{dy} \Big|_{y=0} &= \frac{gV}{(2\pi)^2} \left[1 + (q-1) \frac{m - \mu}{T} \right]^{-\frac{1}{q-1}} \\ &\frac{T^3}{(2q-3)(q-2)} \\ &\left[2 - (q-2) \left(\frac{m - \mu}{T} \right)^2 + 2 \frac{m - \mu}{T} \right. \\ &- 2 \frac{\mu}{T} (2q-3) \left(1 + \frac{m - \mu}{T} \right) \\ &\left. + \frac{\mu^2}{T^2} (2q-3)(q-2) \right]. \quad (13) \end{aligned}$$

This leads to the following expression and generalizes the expression given in [26] to non-zero values of the chemical potential μ (see Appendix A for an outline of the derivation of Eq. (14)):

$$\begin{aligned} \frac{dN}{dp_T dy} \Big|_{y=0} &= \frac{p_T m_T}{T} \frac{dN}{dy} \Big|_{y=0} \left[1 + (q-1) \frac{m_T - \mu}{T} \right]^{-\frac{q}{q-1}} \\ &\times \frac{(2-q)\delta}{(2-q)d^2 + 2dT + 2T^2 + 2\mu\delta(T+d) + \mu^2\delta(2-q)} \\ &\times \left[1 + (q-1) \frac{d}{T} \right]^{\frac{1}{q-1}}. \quad (14) \end{aligned}$$

where the abbreviations $d \equiv m - \mu$ and $\delta \equiv 3 - 2q$ have been used.

In all fits to transverse momentum spectra, the parameter q turns out to be very close to 1 [20,21]. In fact, the value of the non-extensive parameter q for high energy collisions is found to be $1 \leq q \leq 1.2$ [11,27]. In the limit where q is exactly 1, Eq. (12) reduces to the standard exponential function appearing in the Boltzmann distribution. It is therefore useful to expand the above expressions in a Taylor series in $(q-1)$ and see how the deviations from a Boltzmann distribution develop. Such an expansion has been considered previously in [28,29]. The present paper develops a more systematic analysis than the previous ones and considers a slightly different form of the Tsallis distribution, having an extra power of q , because it is consistent with basic thermodynamic relations.

The aim of this paper is to develop a Taylor expansion of Eq. (12) in $(q-1)$ based on the fact that $(q-1) \ll 1$ (see for example [30]). The conditions of validity of such an expansion for pure Tsallis distribution (Eq. (1)) is $|1 - q|E/T < 1$. Apart from this, up to first order in $(q-1)$ an additional condition $|1 - q|(E/T)^2 < 2$ must be satisfied [28]. The condition of validity for expansion up to order $(q-1)^2$ term will be $|1 - q|^2(E/T)^3 < 3$. The expansion to higher orders has also been considered in [31] in the framework of an analysis of quasi-additivity for the Tsallis entropy for different subsystems.

The Taylor expansion is useful as a mathematical tool because it breaks the Tsallis distribution in a series of $(q-1)$ containing powers of energy E . Now, the advantage we get is, it will be easier to consistently include the effect of flow on the Tsallis distribution just by making a substitution $E \rightarrow p^\mu u_\mu$, for a collective four-velocity u^μ of particles with representative four-momentum p^μ [32,33].

There have been earlier attempts to include the effect of collectivity in the dynamics of the particles following the Tsallis distribution in the form of Tsallis-Blast Wave (TBW) formalism [22], or in Refs. [32,34]. In all the cases, an ansatz of fluid four-velocity is taken and energy is replaced by the scalar product $p^\mu u_\mu$. The inclusion of flow inside non-extensive statistics reduces the value of q [35] since some degree of non-extensivity is shared by the dynamics. Also, whenever we have an inhomogeneous thermodynamic system, with regions having different temperatures and exchanging heat with the bigger system, we can define an effective temperature T_{eff} which is affected by energy transfer only when $q \neq 1$ [36,37,38]. The variation of effective temperature with q is seen in [39]. Another important observed phenomenon like m_T scaling is affected by flow. In $p-p$ or $p-A$ collisions, the particle spectra

for different hadrons are having the same slope parameter T and this phenomenon is known as m_T scaling [40]. Due to this scaling behaviour, the particle species cannot be identified just by looking at the spectrum. This behaviour will be manifested in particle distributions following Eq. (12). But, because of the inclusion of collectivity the particle species start having different slope parameters. The average collective velocity as well as the mass of particles will contribute to the slope parameter and hence the scaling is broken [41]. It is possible that q represents the joint action of many dynamical factors [42] and it cannot be excluded at present that when these are accounted for, the factor $q - 1$ could well become zero. The values of the parameters are clearly sensitive to the details of the hadronization mechanism [43, 44].

The TBW formalism considers an implicit dependence of fluid rapidity on the velocity; but in the present case we consider a cylindrical geometry and velocity comes explicitly in the calculations. In contrast to the numerical treatment in [22], we provide an analytical formula for the Tsallis distribution expanded up to $\mathcal{O}(q-1)$ in presence of flow. In the next section, we derive the Taylor expansion for the Tsallis distribution in the series of $(q-1)$ and we compare the order by order deviation from a thermalized Boltzmann distribution of transverse momentum spectra in hadronic and nuclear collisions. In Sec. 4 we find out the expressions for number density (n), pressure (P) and energy density (ϵ) for a system with non-zero chemical potential (μ). We verify the thermodynamic relationship $n = \partial P / \partial \mu$. In Sec. 5 we derive an analytical formula including flow up to $\mathcal{O}(q-1)$ of a Taylor series expansion of the Tsallis distribution and show its application to experimental data. Finally we summarize the paper in Sec. 6.

3 Momentum Distributions to First and Second Order in $(q-1)$

Assuming the parameter q to be close to 1, as is the value for many cases in high energy physics, the modified Tsallis distribution, f^q , appearing in the expressions for the thermodynamic quantities can be expanded in a Taylor series in $q-1$ with the following result (see appendix B for a detailed derivation):

$$\begin{aligned} & \left[1 + (q-1) \frac{E-\mu}{T} \right]^{-\frac{q}{q-1}} \\ & \simeq e^{-\frac{E-\mu}{T}} \left\{ 1 + (q-1) \frac{1}{2} \frac{E-\mu}{T} \left(-2 + \frac{E-\mu}{T} \right) \right. \\ & + \frac{(q-1)^2}{2!} \frac{1}{12} \left[\frac{E-\mu}{T} \right]^2 \left[24 - 20 \frac{E-\mu}{T} + 3 \left(\frac{E-\mu}{T} \right)^2 \right] \\ & + \mathcal{O} \{ (q-1)^3 \} \\ & + \dots \} \end{aligned} \quad (15)$$

This result can be used for the invariant yield of particles if it is written in terms of the Tsallis distribution,

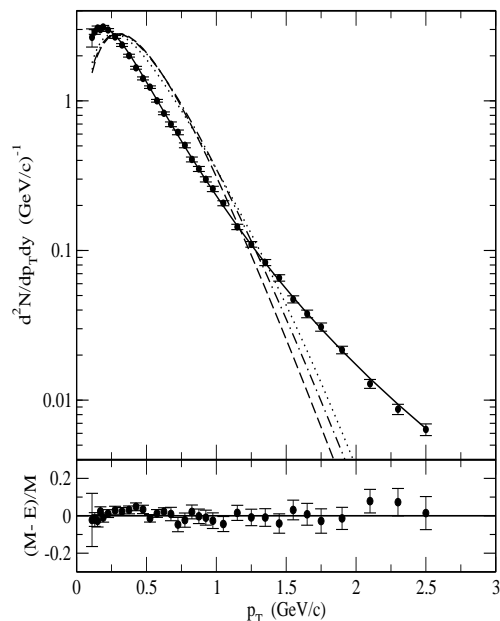


Fig. 1. Fits to the normalized differential yields of π^+ as measured by the ALICE collaboration in $p-p$ collisions at $\sqrt{s} = 0.9$ TeV [6] fitted with the Tsallis (solid line) and Boltzmann distributions (dashed line). Also shown are fits with the Tsallis distribution keeping terms to first (dash-dotted line) and second order in $(q-1)$ (dotted line). The lower part of the figure shows the difference between model (M) and experiment (E) normalized to the model (M) values.

$$E \frac{dN}{d^3p} = CE \left[1 + (q-1) \frac{E-\mu}{T} \right]^{-\frac{q}{q-1}} \quad (16)$$

where $C \equiv gV/(2\pi)^3$. Let us use the following notations: $(q-1) \equiv x$; $(E-\mu)/T = \Phi$ and $1 + (q-1) \frac{E-\mu}{T} = 1 + x\Phi = f(x)$. Hence, the expansion of the Tsallis distribution up to $\mathcal{O}(x^2)$ can be written as:

$$\begin{aligned} E \frac{dN}{d^3p} & \simeq CE e^{-\Phi} + CE \frac{x\Phi}{1!} (-2 + \Phi) e^{-\Phi} \\ & + CE \frac{x^2\Phi^2}{2!} (24 - 20\Phi + 3\Phi^2) e^{-\Phi} \end{aligned} \quad (17)$$

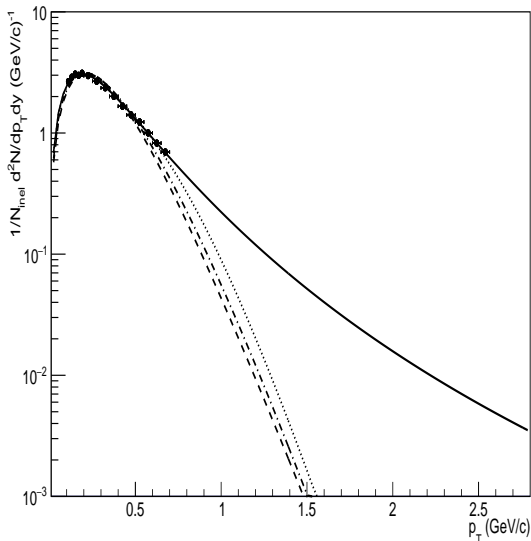


Fig. 2. Fits to the normalized differential yields of π^+ , including only results at small values of the transverse momentum, as measured by the ALICE collaboration in $p-p$ collisions at $\sqrt{s} = 0.9$ TeV [6] fitted with the Tsallis (solid line) and Boltzmann distributions (dashed line). Also shown are fits with the Tsallis distribution keeping terms to first (dash-dotted line) and second order in $(q-1)$ (dotted line).

Hence one obtains

$$\begin{aligned} \frac{dN}{p_T dp_T dy d\phi} &\simeq CE e^{-\Phi} + CE \frac{x}{1!} \frac{\Phi}{2} (-2 + \Phi) e^{-\Phi} \\ &+ CE \frac{x^2}{2!} \frac{\Phi^2}{12} (24 - 20\Phi + 3\Phi^2) e^{-\Phi} \quad (18) \end{aligned}$$

Since, we use a modified form of Tsallis distribution, a comparison with similar work will be worthwhile at this point. With this aim, we integrate over the rapidity variable to compare the transverse mass spectrum obtained from the present approach with that obtained in Ref. [29]:

$$\begin{aligned} \frac{dN}{m_T dm_T} &= \frac{gV}{2\pi^2} m_T \left[K_1 \left(\frac{m_T}{T} \right) e^{\frac{\mu}{T}} \right. \\ &- \frac{q-1}{2} \frac{m_T}{T} \left\{ K_0 \left(\frac{m_T}{T} \right) + K_2 \left(\frac{m_T}{T} \right) \right\} \\ &+ \frac{q-1}{8} \left(\frac{m_T}{T} \right)^2 \left\{ K_3 \left(\frac{m_T}{T} \right) + 3K_1 \left(\frac{m_T}{T} \right) \right\} \\ &+ \frac{\mu(q-1)}{T} K_1 \left(\frac{m_T}{T} \right) + \frac{\mu^2(q-1)}{2T^2} K_1 \left(\frac{m_T}{T} \right) \\ &\left. - \frac{\mu m_T (q-1)}{2T^2} \left\{ K_0 \left(\frac{m_T}{T} \right) + K_2 \left(\frac{m_T}{T} \right) \right\} \right] \\ &+ \mathcal{O}((q-1)^2) + \dots \quad (19) \end{aligned}$$

where K_n s are the modified Bessel's functions of second kind (see Appendix E). In principle, while examining the transverse spectra, the rapidity integration should be within a maximum value y_{max} , say. But, owing to the presence of the term $e^{-m_T \cosh y/T}$, the integrand drops down very

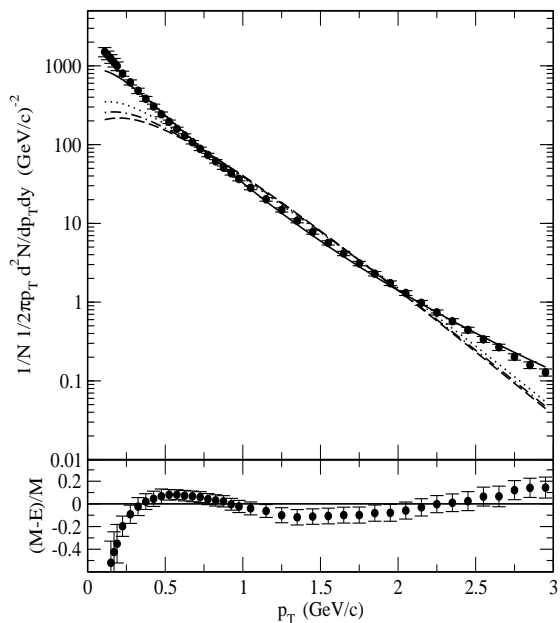


Fig. 3. Fits to the normalized differential π^- yields as measured by the ALICE collaboration in (0–5)% Pb-Pb collisions at $\sqrt{s_{NN}} = 2.76$ TeV [10] fitted with the Tsallis (solid line) and Boltzmann distributions (dashed line). Also shown are fits with the Tsallis distribution keeping terms to first (dash-dotted line) and second order in $(q-1)$ (dotted line). The lower part of the figure shows the difference between model (M) and experiment (E) normalized to the model (M) values.

fast with increasing y . And so, according to the standard practice, we can effectively replace the rapidity integration from 0 to y_{max} to 0 to ∞ so that the integration yields Bessel functions. The first term in the above expression is the well-known formula for a thermal source with a Boltzmann distribution:

$$\frac{dN}{p_T dp_T} = \frac{gV}{2\pi^2} m_T e^{\frac{\mu}{T}} K_1 \left(\frac{m_T}{T} \right) \quad (20)$$

In the limit $\mu = 0$, the transverse mass spectrum obtained from Ref. [29] (up to $\mathcal{O}(q-1)$) does not contain the term involving K_0 and K_2 .

The Boltzmann distribution, the pure Tsallis distribution (Eq. (12)) and the expansion of the Tsallis distri-

bution up to the first and second order of $(q - 1)$ (Eq. (18)) were used to fit the transverse momentum distributions obtained by the ALICE collaboration. The results are shown in Fig. 1 for p-p collisions at $\sqrt{s} = 0.9$ TeV and in Fig. 3 for Pb-Pb collisions at $\sqrt{s_{NN}} = 2.76$ TeV. It is well known that the Tsallis fits give excellent results for p-p collisions but are not very good for Pb-Pb collisions as can be seen clearly in Fig. (2) where a large deviation at small p_T is seen.

It can be seen from the fits to the p - p distribution that the successive terms in $(q - 1)$ improve the fits but not in a convincing manner. Clearly, it is the best to use the full Tsallis distribution and not the series expansion. It might turn out of course that the series expansion could be of use in a different situation where the comparison with a Boltzmann distribution is more relevant.

The fits in the figures were done using the MINUIT package with the following numerical results.

In Fig. 1 we show fits to the transverse momentum distribution of π^+ in p-p collisions at 900 GeV. For the plain Tsallis distribution (solid line) the parameters were obtained as being $T = 70.8$ MeV, $q = 1.1474$. The volume V was determined as corresponding to a spherical radius of 4.81 fm. For the Boltzmann distribution (dashed line) the parameters were determined as being $T = 150.2$ MeV, while the radius used to determine the volume was fixed at a value of 2.65 fm. For the fit using the Boltzmann distribution and the first order term in $(q - 1)$ (dashed-dotted line) the values are $T = 138.4$ MeV, $q = 1.035$ while the radius is given by 2.80 fm. In the last case corresponding to Boltzmann plus first and second orders in $(q - 1)$ (dotted line) one has $T = 121.2$ MeV, $q = 1.065$ and a radius of 3.09 fm. As is well-known and evident, the fit using the Tsallis distribution is very good.

In Fig. 2 we show fits to the small transverse momentum region of π^+ in p-p collisions at 900 GeV. In this case the fits using the Boltzmann distribution are fairly good. The deviation with the Tsallis distribution becomes very prominent only for larger transverse momenta. For the plain Tsallis distribution (solid line) the parameters were obtained as being $T = 70.8$ MeV, $q = 1.145$, similar to the full range of p_T . The volume V was determined as corresponding to a spherical radius of 4.82 fm. For the Boltzmann distribution (dashed line) the parameters were determined as being $T = 104.9$ MeV, i.e. much lower than the full range in p_T while the radius used to determine the volume was fixed at a value of 3.61 fm. For the fit using the Boltzmann distribution and the first order term in $(q - 1)$ (dashed-dotted line) the values are $T = 89.9$ MeV, $q = 1.07$ while the radius is given by 4.03 fm. In the last case corresponding to Boltzmann plus first and second orders in $(q - 1)$ (dotted line) one has $T = 77$ MeV, $q = 1.11$ and a radius of 4.54 fm.

In Fig. 3 we show fits to the normalized differential π^- yields in $(0 - 5)\%$ Pb-Pb collisions at $\sqrt{s_{NN}} = 2.76$ TeV as measured by the ALICE collaboration [10] with the Tsallis (solid line) and Boltzmann distributions (dashed line). Also shown are fits with the Tsallis distribution keeping terms to first order (dash-dotted line) and second order in

$(q - 1)$ (dotted line). The lower part of the figure shows the difference between the Tsallis distribution (M) and experiment (E). It is clear that the best fit is achieved with the full Tsallis distribution, whereas, using the Boltzmann distribution the description is not good. Successive corrections in $(q - 1)$ improve the description. There is a clear deviation at very low transverse momentum (below 0.5 GeV) and also at higher values above 2.75 GeV.

4 Thermodynamic Quantities to First Order in $(q - 1)$

The particle density in Tsallis thermodynamics is given to first order in $(q - 1)$ by the following expression:

$$n^B + (q - 1)n^1 \quad (21)$$

where n^B is the standard Boltzmann result for the particle density:

$$n^B = \frac{g}{2\pi^2} e^{\frac{\mu}{T}} T^3 a^2 K_2(a), \quad (22)$$

with $a \equiv m/T$, and the first order expression in $q - 1$ is given by

$$\begin{aligned} n^1 = \frac{ge^{\frac{\mu}{T}} T^3}{4\pi^2} & [-6a^2 K_2(a) - 2a^3 K_1(a) \\ & - 4a^2 b K_2(a) + 3a^3 K_3(a) + a^4 K_2(a) + a^2 b^2 K_2(a) \\ & - 2a^3 b K_1(a)]. \end{aligned} \quad (23)$$

In Fig. 4 we show the ratio of the particle density to first order in $(q - 1)$ to the full particle density as given by the Tsallis distribution, $(n^B + (q - 1)n^1)/n$ for several values of q indicated in the figure as a function of the temperature T .

It can be seen that the expansion in $(q - 1)$ is excellent if $(q - 1) = 0.01$ but rapidly deviates from the full Tsallis distribution for larger values of q . Already for $(q - 1) \approx 0.1$ the deviations are of the order of 10 % as can be seen from Fig. 4.

For comparison we show in Fig. 5, the first order expansion compared to the Boltzmann expression, $(n^B + (q - 1)n^1)/n^B$, again as a function of the temperature T for several values of the parameter q . In this case the deviations are most pronounced for small values of the temperature.

Correspondingly, the energy density is obtained as:

$$\epsilon^B + (q - 1)\epsilon^1 \quad (24)$$

$$\epsilon^B = \frac{ge^{\frac{\mu}{T}} T^4}{2\pi^2} (3a^2 K_2(a) + a^3 K_1(a)) \quad (25)$$

$$\begin{aligned} \epsilon^1 = \frac{ge^{\frac{\mu}{T}} T^4}{4\pi^2} & [9a^3 K_3(a) + 4a^4 K_2(a) + a^5 K_1(a) \\ & + 2b (3a^2 K_2(a) + a^3 K_1(a) - 3a^3 K_3(a) + a^4 K_2(a)) \\ & + b^2 (3a^2 K_2(a) + a^3 K_1(a))] \end{aligned} \quad (26)$$

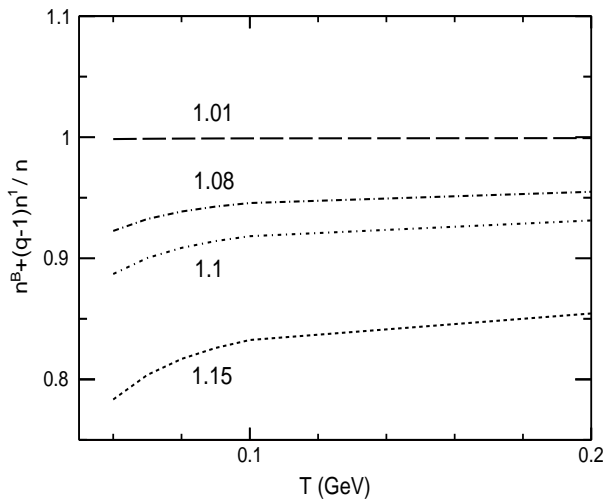


Fig. 4. The ratio of the particle density calculated to first order in $(q - 1)$ normalized to the particle density of a Tsallis gas as a function of the temperature for different values of the parameter q . The mass is taken as being the pion mass. The values of the parameter q are 1.01 for the dashed line, 1.08 for the dot-(long)dashed line, 1.1 for the dot-(short)dashed line and 1.15 for the dotted line.

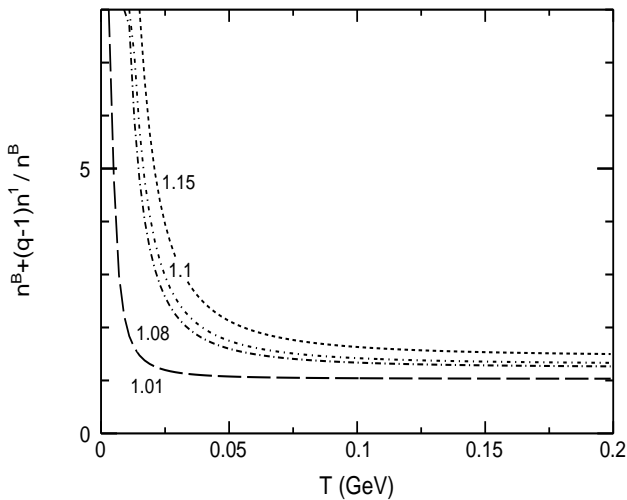


Fig. 5. The ratio of the particle density calculated to first order in $(q - 1)$ normalized to the particle density of a Boltzmann gas as a function of the temperature for different values of the parameter q . The mass is taken as being the pion mass. The values of the parameter q are 1.01 for the dashed line, 1.08 for the dot-(long)dashed line, 1.1 for the dot-(short)dashed line and 1.15 for the dotted line.

In Fig. 6 we show the ratio of the energy density to first order in $(q - 1)$ to the full energy density as given by the Tsallis distribution, $(\epsilon^B + (q - 1)\epsilon^1)/\epsilon$ for several values of q indicated in the figure as a function of the temperature T .

Again, as noted previously for the particle density, it can be seen that the expansion in $(q - 1)$ is excellent if $(q - 1) =$

0.01 but rapidly deviates from the full Tsallis distribution for larger values of q . Also here, for $(q - 1) \approx 0.1$ the deviations are of the order of 20 % as can be seen from Fig. 6. For comparison we show in Fig. 7, the first

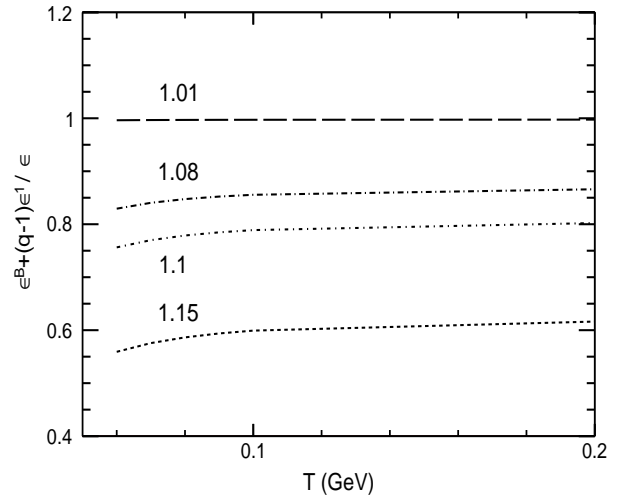


Fig. 6. The ratio of the energy density calculated to first order in $(q - 1)$ normalized to the energy density of a Tsallis gas as a function of the temperature for different values of the parameter q . The mass is taken as being the pion mass. The values of the parameter q are 1.01 for the dashed line, 1.08 for the dot-(long)dashed line, 1.1 for the dot-(short)dashed line and 1.15 for the dotted line.

order expansion compared to the Boltzmann expression, $(\epsilon^B + (q - 1)\epsilon^1)/\epsilon^B$, as a function of the temperature T for several values of the parameter q . As in the previous case the deviations are most pronounced for small values of the temperature. Finally, the pressure is given by

$$P^B + (q - 1)P^1 \quad (27)$$

$$P^B = \frac{ge^{\frac{\mu}{T}}T^4 a^2 K_2(a)}{2\pi^2} \quad (28)$$

$$P^1 = \frac{ge^{\frac{\mu}{T}}T^4}{4\pi^2} [a^4 K_2(a) + 3a^3 K_3(a) - 2a^3 b K_3(a) + a^2 b^2 K_2(a) + 2a^2 b K_2(a)] \quad (29)$$

In Fig. 8 we show the ratio of the pressure to first order in $(q - 1)$ to the full pressure as given by the Tsallis distribution, $(P^B + (q - 1)P^1)/P$ for several values of q indicated in the figure as a function of the temperature T . Again, as noted previously, it can be seen that the expansion in $(q - 1)$ is excellent if $(q - 1) = 0.01$ but rapidly deviates from the full Tsallis distribution for larger values of q . Also here, for $(q - 1) \approx 0.1$ the deviations are of the order of 20 % as can be seen from Fig. 8. Again, we show in Fig. 9, the first order expansion compared to the Boltzmann expression, $(P^B + (q - 1)P^1)/P^B$, as a function of

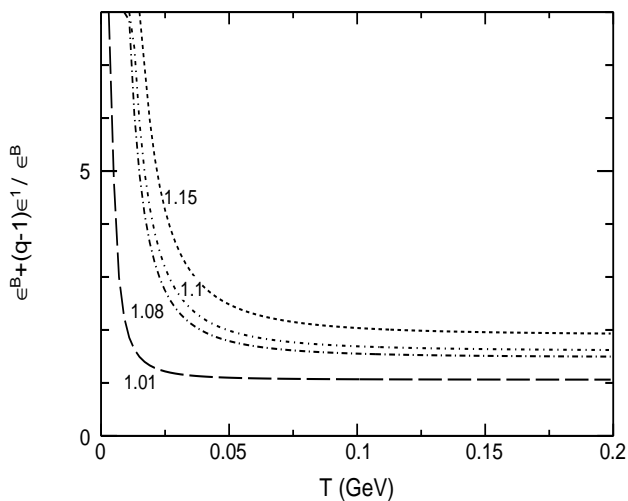


Fig. 7. The ratio of the energy density calculated to first order in $(q-1)$ normalized to the energy density of a Boltzmann gas as a function of the temperature for different values of the parameter q .

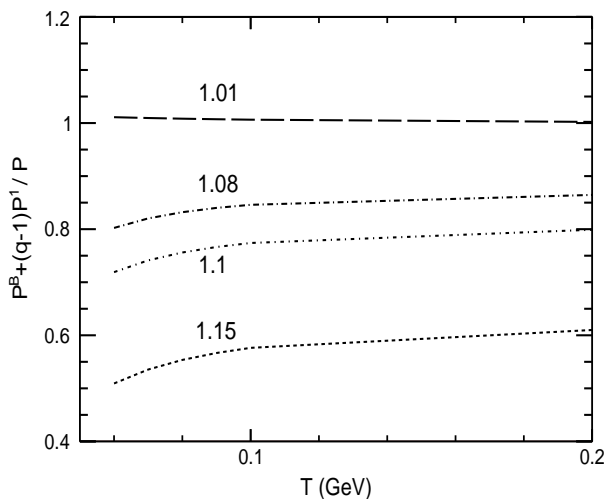


Fig. 8. The ratio of the pressure calculated to first order in $(q-1)$ normalized to the pressure of a Tsallis gas as a function of the temperature for different values of the parameter q .

the temperature T for several values of the parameter q . In this case the deviations are most pronounced for small values of the temperature.

The entropy density can be obtained from the above expressions by using the thermodynamic relation

$$\epsilon + P = Ts + \mu n \quad (30)$$

and is not being shown here.

Before closing the section, we comment about the validity of the present expansion up to the second order in $(q-1)$. As we have already seen, for truncation of the expansion up to the first order with pure Tsallis distribution,

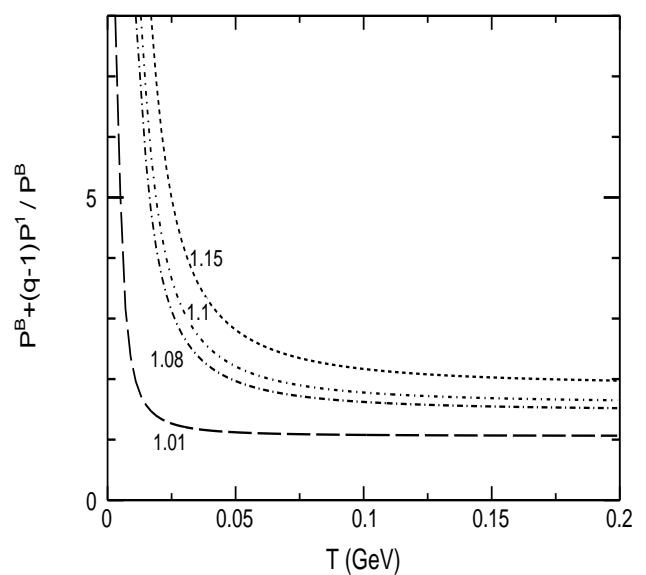


Fig. 9. The ratio of the pressure calculated to first order in $(q-1)$ normalized to the pressure of a Boltzmann gas as a function of the temperature for different values of the parameter q .

one needs to satisfy two conditions, i.e.

$$|1 - q| \frac{E}{T} < 1 \quad (31)$$

and

$$|1 - q| \left(\frac{E}{T} \right)^2 < 2 \quad (32)$$

With the thermodynamically consistent Tsallis distribution, the second condition turns out to be $|q(1-q)|(E/T)^2 < 2$. For expansion up to second order in $(q-1)$ with modified Tsallis distribution, the condition becomes $q^2|1-q|(E/T)^3 < 3$.

Given the two values (the highest and the lowest) of $(q-1)$ used in the present analysis, we want to put an upper bound in E/T until which the expansion will be reliable. If $(q-1) = 0.15$, Eq.(31) gives $E/T < 6.7$ and the modified condition for expansion up to first order gives $(E/T)^2 < 11.59$. That means for $T = 0.1$ GeV, the expansion will be reliable up to $E \approx 0.3$ GeV when $(q-1) = 0.15$.

If $(q-1) = 0.01$, Eq.(31) gives $E/T < 100$ and the modified condition for expansion up to first order gives $(E/T)^2 < 198$. That means for $T = 0.1$ GeV, the expansion will be reliable up to $E \approx 1.4$ GeV when $(q-1) = 0.01$. The permissible values of $(q-1)$ and E/T for reliable expansion up to the second order in $(q-1)$ are shown to reside inside the smaller area filled with slanted lines. This is shown in Fig. 10.

Hence, we conclude from the above discussion that the smaller the q value the more reliable the expansion becomes.

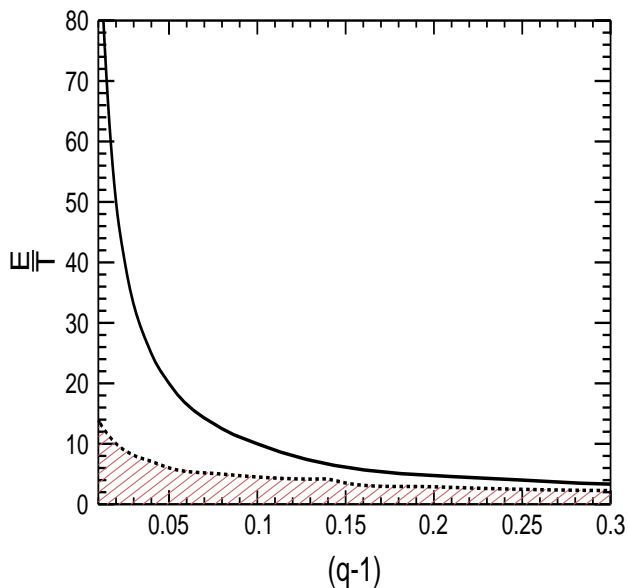


Fig. 10. (colour online) The region of validity for the expansion in $(q-1)$ up to second order. The area under the solid line denotes the region where only the condition $|1-q|E/T < 1$ is satisfied. The common overlapped area (i.e. the area under the dotted line) depicts the region within which all the conditions for expansion up to second order are satisfied.

5 Inclusion of Flow to First Order in $(q-1)$

In order to see how the inclusion of flow could improve the description of the transverse momentum distributions obtained in Pb-Pb collisions, we have included a constant flow velocity, β . Assuming space-like freeze-out surface, the invariant yield is given by (see Appendix for the derivation).

$$\frac{1}{p_T} \frac{dN}{dp_T dy} = \frac{gV}{(2\pi)^2} \left\{ \begin{aligned} & 2Tr^2 I_0(s) K_1(r) - s I_1(s) K_0(r) \\ & -(q-1) T r^2 I_0(s) [K_0(r) + K_2(r)] \\ & + 4(q-1) T r s I_1(s) K_1(r) \\ & -(q-1) T s^2 K_0(r) [I_0(s) + I_2(s)] \\ & + \frac{(q-1)}{4} T r^3 I_0(s) [K_3(r) + 3K_1(r)] \\ & - \frac{3(q-1)}{2} T r^2 s [K_2(r) + K_0(r)] I_1(s) \\ & + \frac{3(q-1)}{2} T s^2 r [I_0(s) + I_2(s)] K_1(r) \\ & - \frac{(q-1)}{4} T s^3 [I_3(s) + 3I_1(s)] K_0(r) \end{aligned} \right\} \quad (33)$$

where

$$r \equiv \frac{\gamma m_T}{T} \quad (34)$$

$$s \equiv \frac{\gamma v p_T}{T} \quad (35)$$

$I_n(s)$ and $K_n(r)$ are the modified Bessel functions of the first and second kind. Now, in this formula, the freeze-out surface has been considered to be space-like and so the integration over the freeze-out surface turns out to be trivial. For a more detailed treatment of the freeze-out surface in this context, the readers are referred to Ref. [34].

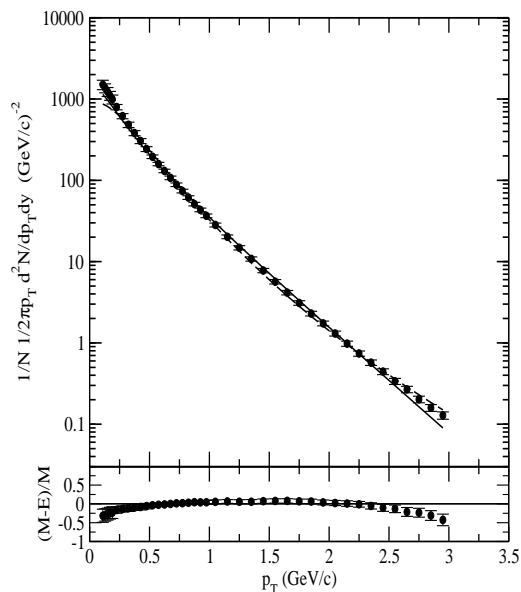


Fig. 11. Fits to the normalized differential π^- yields as measured by the ALICE collaboration in (0–5)% Pb-Pb collisions at $\sqrt{s_{NN}} = 2.76$ TeV [10]. The fit with the Tsallis distribution including flow keeping terms to first order in $(q-1)$ (dashed line). The flow velocity is fixed at $\beta = 0.609$, with $T = 146$ MeV, $q = 1.030$ and the radius of the volume is $R = 29.8$ fm. The solid line is the Tsallis distribution without flow as given in Fig. 3. The lower part of the figure shows the difference between model (M), i.e. Tsallis with flow up to first order in $(q-1)$, and experiment (E) normalized to the model (M) values.

The comparison between model and experiment is quite good with notable deviations at small values of the transverse momentum p_T and again above values of 2.5 GeV

(see Fig. 11). These could easily be attributed to the coarse way of treating transverse flow. More detailed investigations have been carried out in [22].

6 Summary and Conclusion

The Tsallis distribution describes extremely well the transverse momentum distributions in p-p collisions at high energies. All fits performed so far show that the parameter q is always close to 1. In view of this, we have presented in this paper a series expansion of quantities relevant in the analysis of high energy physics in $(q-1)$. The Tsallis distribution itself has been obtained to second order in $(q-1)$. A rough comparison with experimental data has been done for the transverse momentum distributions obtained in p-p collisions. In the case of Pb-Pb collisions we have given an estimate using flow with a fixed flow velocity. In most cases the series expansion turns out not to be a useful description of transverse momentum distributions but it could be useful in analyses where a comparison and detailed investigation is needed when comparing the Tsallis and the Boltzmann distributions. Furthermore, a systematic study of the identified particle yield due to $p-p$ and heavy-ion collision at RHIC and LHC has been done in [35] where the flow formula (Eq. (33)) has been used to fit the spectra.

Acknowledgement

The authors would like to thank Dr. Prakhar Garg, IIT Indore for useful discussions and help during the preparation of the manuscript. We thank the referees for their helpful comments which improved the paper.

Appendix

A Derivation of Eq. (13) and Eq. (14)

The result quoted in Eq. (13) can be obtained by a change of variable from p_T to x which is defined by

$$x \equiv 1 + (q-1) \frac{m_T - \mu}{T}. \quad (36)$$

This leads to the following integral

$$\begin{aligned} \left. \frac{dN}{dy} \right|_{y=0} &= \int_0^\infty dp_T \left. \frac{dN}{dp_T dy} \right|_{y=0} \\ &= \frac{gV}{(2\pi)^2} \int_0^\infty dp_T p_T m_T \left[1 + (q-1) \frac{m_T - \mu}{T} \right]^{-\frac{q}{q-1}} \\ &= \frac{gV}{(2\pi)^2} \frac{T}{q-1} \int_a^\infty dx x^{-\frac{q}{q-1}} \left[\frac{x-1}{q-1} T + \mu \right]^2 \end{aligned} \quad (37)$$

with

$$a \equiv 1 + (q-1) \frac{m - \mu}{T} \quad (38)$$

This is an elementary integral over a polynomial function. The result is

$$\begin{aligned} \left. \frac{dN}{dy} \right|_{y=0} &= \frac{gV}{(2\pi)^2} \left[1 + (q-1) \frac{m - \mu}{T} \right]^{-\frac{1}{q-1}} \\ &\left\{ \frac{T^3}{(2q-3)(q-2)} \left[2 - (q-2) \left(\frac{m - \mu}{T} \right)^2 + 2 \frac{m - \mu}{T} \right] \right. \\ &\left. - 2 \frac{T^2 \mu}{q-2} \left[1 + \frac{m - \mu}{T} \right] + T \mu^2 \right\} \end{aligned} \quad (39)$$

This makes it possible to express the volume V in terms of $\left. \frac{dN}{dy} \right|_{y=0}$ from Eq. (13) in the text. Replacing the volume term in Eq. (12) in terms of Eq. (39), we get Eq. (14).

B Expansion in $(q-1)$ of Tsallis distribution

The Taylor expansion is done efficiently by the following change of variables:

$$q-1 \equiv x; \quad \frac{E - \mu}{T} \equiv \Phi \quad (40)$$

$$1 + (q-1) \frac{E - \mu}{T} \equiv 1 + x \Phi \equiv f(x) \quad (41)$$

$$-\frac{q}{q-1} = -\frac{1+x}{x} \equiv g(x) \quad (42)$$

The relevant distribution function can then be written as

$$\begin{aligned} \left[1 + (q-1) \frac{E - \mu}{T} \right]^{-\frac{q}{q-1}} &= [1 + x\Phi]^{-\frac{1+x}{x}} \\ &= f(x)^{g(x)} \\ &= \mathcal{F}(x) \end{aligned} \quad (43)$$

Expanding $\mathcal{F}(x)$ in Taylor series about $x=0$, we get

$$\mathcal{F}(x=0) = e^{-\Phi} \quad (44)$$

$$\left. \frac{d\mathcal{F}(x)}{dx} \right|_{x=0} = \frac{1}{2} (-2 + \Phi) \Phi e^{-\Phi} \quad (45)$$

$$\left. \frac{d^2\mathcal{F}(x)}{dx^2} \right|_{x=0} = \frac{\Phi^2}{12} (24 - 20\Phi + 3\Phi^2) e^{-\Phi} \quad (46)$$

for $\mathcal{O}(x^0)$, $\mathcal{O}(x)$ and $\mathcal{O}(x^2)$ respectively. The final results can be summarized in the following equation

$$\begin{aligned} & \left[1 + (q-1) \frac{E-\mu}{T} \right]^{-\frac{q}{q-1}} \\ & \simeq e^{-\frac{E-\mu}{T}} \\ & + (q-1) \frac{1}{2} \frac{E-\mu}{T} \left(-2 + \frac{E-\mu}{T} \right) e^{-\frac{E-\mu}{T}} \\ & + \frac{(q-1)^2}{2!} \frac{1}{12} \left[\frac{E-\mu}{T} \right]^2 \\ & \times \left[24 - 20 \frac{E-\mu}{T} + 3 \left(\frac{E-\mu}{T} \right)^2 \right] e^{-\frac{E-\mu}{T}} \\ & + \dots \end{aligned} \quad (47)$$

For completeness we also quote the following result

$$\begin{aligned} & \left[1 + (q-1) \frac{E-\mu}{T} \right]^{-\frac{1}{q-1}} \\ & \simeq e^{-\frac{E-\mu}{T}} \\ & + (q-1) \frac{1}{2} \left(\frac{E-\mu}{T} \right)^2 e^{-\frac{E-\mu}{T}} \\ & + \frac{(q-1)^2}{2!} \frac{1}{12} \left[\frac{E-\mu}{T} \right]^2 \\ & \times \left[-8 \left(\frac{E-\mu}{T} \right) + 3 \left(\frac{E-\mu}{T} \right)^2 \right] e^{-\frac{E-\mu}{T}} \\ & + \dots \end{aligned} \quad (49)$$

C Tsallis Thermodynamics

C.1 Particle number density n

Up to $\mathcal{O}(q-1)$, the number density can be written as:

$$\begin{aligned} n &= \frac{g}{(2\pi)^3} \int d^3p \left[e^{-\frac{E-\mu}{T}} + (q-1) \frac{E-\mu}{2T} \right. \\ & \left. \left(-2 + \frac{E-\mu}{T} \right) e^{-\frac{E-\mu}{T}} \right] \end{aligned} \quad (50)$$

We define,

$$\begin{aligned} p^2 + m^2 &= E^2; \\ \frac{E}{T} = \omega, \frac{m}{T} &= a, \frac{\mu}{T} = b \end{aligned} \quad (51)$$

And hence,

$$\begin{aligned} n &= n^B + \frac{g(q-1)e^{\frac{\mu}{T}}T^3}{4\pi^2} \int d\omega \omega (\omega^2 - a^2)^{\frac{1}{2}} \\ & (-2\omega + 2b + \omega^2 + b^2 - 2\omega b) e^{-\omega} \\ n &= n^B + \frac{g(q-1)e^{\frac{\mu}{T}}T^3}{4\pi^2} [-6a^2K_2(a) - 2a^3K_1(a) \\ & - 4a^2bK_2(a) + 3a^3K_3(a) + a^4K_2(a) + a^2b^2K_2(a) \\ & - 2a^3bK_1(a)] \end{aligned} \quad (52)$$

Here the following form of the modified Bessel function of second kind [45] is used:

$$K_n(a) = \frac{2^{n-1}(n-1)!}{(2n-2)!a^n} \int_a^\infty d\omega \omega (\omega^2 - a^2)^{n-\frac{3}{2}} e^{-\omega} \quad (53)$$

On the other hand, by using Boltzmann Statistics one obtains,

$$n^B = \frac{ge^{\frac{\mu}{T}}T^3a^2K_2(a)}{2\pi^2} \quad (54)$$

C.2 Pressure

To first order in $(q-1)$ the pressure is given by:

$$\begin{aligned} P &= \frac{g}{(2\pi)^3} \int d^3p \frac{p^2}{3E} \left[e^{-\frac{E-\mu}{T}} + (q-1) \frac{E-\mu}{2T} \right. \\ & \left. \left(-2 + \frac{E-\mu}{T} \right) e^{-\frac{E-\mu}{T}} \right] \end{aligned} \quad (55)$$

Using the same definitions as in Eq. (51), we get

$$\begin{aligned} P &= P^B + \frac{g(q-1)e^{\frac{\mu}{T}}T^4}{12\pi^2} \int d\omega (\omega^2 - a^2)^{\frac{3}{2}} \\ & (-2\omega + 2b + \omega^2 + b^2 - 2\omega b) e^{-\omega} \\ & = P^B + \frac{g(q-1)e^{\frac{\mu}{T}}T^4}{4\pi^2} [a^4K_2(a) + 3a^3K_3(a) \\ & - 2a^3bK_3(a) + a^2b^2K_2(a) + 2a^2bK_2(a)] \end{aligned} \quad (56)$$

Using Eq. (51) along with Eq. (53) as well as another representation of the modified Bessel function,

$$K_n(a) = \frac{2^n n!}{(2n)! a^n} \int_a^\infty d\omega (\omega^2 - a^2)^{n-\frac{1}{2}} e^{-\omega} \quad (57)$$

Eq. (53) can be obtained from Eq. (57) by dint of partial integration. The Boltzmann pressure density is, similarly given by:

$$P^B = \frac{ge^{\frac{\mu}{T}}T^4a^2K_2(a)}{2\pi^2} \quad (58)$$

C.3 Energy density ϵ

$$\epsilon = \frac{g}{(2\pi)^3} \int d^3p E \left[e^{-\frac{E-\mu}{T}} + (q-1) \frac{E-\mu}{2T} \left(-2 + \frac{E-\mu}{T} \right) e^{-\frac{E-\mu}{T}} \right] \quad (59)$$

Using Eq. (51) along with Eq. (53),

$$\begin{aligned} \epsilon = \epsilon^B + \frac{g(q-1)e^{\frac{\mu}{T}}T^4}{4\pi^2} & [9a^3K_3(a) + 4a^4K_2(a) + a^5K_1(a) \\ & + 2b(3a^2K_2(a) + a^3K_1(a) - 3a^3K_3(a) + a^4K_2(a)) \\ & + b^2(3a^2K_2(a) + a^3K_1(a))] \end{aligned} \quad (60)$$

with

$$\epsilon^B = \frac{ge^{\frac{\mu}{T}}T^4}{2\pi^2} (3a^2K_2(a) + a^3K_1(a)) \quad (61)$$

C.4 Checking Thermodynamic Consistency

We know that for thermodynamic variables n and P at non-zero μ we have,

$$\begin{aligned} n &= \partial P / \partial \mu \quad (62) \\ n^B + (q-1)n^1 + \dots &= \partial P^B / \partial \mu + \\ & (q-1)\partial P^1 / \partial \mu + \dots \end{aligned} \quad (63)$$

where the superscripts denote the order of $(q-1)$ in the expansion. Since the terms in the expansion are linearly independent, the identity given by Eq. (62) is to be satisfied at every order of $(q-1)$. Since our expansion is up to $\mathcal{O}(q-1)$, we will check the identity for that order now. Rearranging and reordering the $\mathcal{O}(q-1)$ terms in Eq. (52) we get,

$$\begin{aligned} n^1 &= \frac{ge^{\frac{\mu}{T}}T^3}{4\pi^2} [a^3K_3(a) + a^4K_2(a) \\ & - 4a^2bK_2(a) + 2a^3b(K_3(a) - K_1(a)) \\ & - 2a^3bK_3(a) + a^2b^2K_2(a) - 6a^2K_2(a) \\ & + 2a^3(K_3(a) - K_1(a))] \end{aligned} \quad (64)$$

Using the recursion relation for the modified Bessel's functions,

$$K_{n+1}(a) - K_{n-1}(a) = \frac{2n}{a} K_n(a) \quad (65)$$

$$\begin{aligned} n^1 &= \frac{g(q-1)e^{\frac{\mu}{T}}T^3}{4\pi^2} [a^3K_3(a) + a^4K_2(a) \\ & + 4a^2bK_2(a) - 2a^3bK_3(a) + a^2b^2K_2(a) \\ & + 2a^2K_2(a)] \\ &= \frac{\partial P^1}{\partial \mu} \end{aligned} \quad (66)$$

Hence, proved.

D Momentum Distribution

The invariant particle yield is given by,

$$E \frac{dN}{d^3p} = CE \left[1 + (q-1) \frac{E-\mu}{T} \right]^{-\frac{q}{q-1}} \quad (67)$$

Where $C = \frac{gV}{(2\pi)^3}$. Assuming $q-1 \ll 1$ we are to expand it in Taylor series. Let,

$$\begin{aligned} \frac{dN}{p_T dp_T dy d\phi} &= CE \left[e^{-\Phi} + \frac{x}{1!} \frac{1}{2} (-2 + \Phi) \Phi e^{-\Phi} \right. \\ & \left. + \frac{x^2}{2!} \frac{\Phi^2}{12} (24 - 20\Phi + 3\Phi^2) e^{-\Phi} + \dots \right] \end{aligned} \quad (68)$$

where y is rapidity and ϕ is the azimuthal angle of emission. Now, parameterizing energy E in terms of rapidity y i.e. putting $E = m_T \cosh y$ and integrating over y we get Eq. (19).

E Flow in Tsallis Distribution

We use the following ansatz (in cylindrical polar coordinates) for introducing flow inside our calculations:

$$p^\mu = (m_T \cosh y, p_T \cos \phi, p_T \sin \phi, m_T \sinh y) \quad (69)$$

$$u^\mu = (\gamma \cosh \zeta, \gamma v \cos \alpha, \gamma v \sin \alpha, \gamma \sinh \zeta) \quad (70)$$

where $(\zeta)y$ is the (space-time)rapidity of particles (fluid-element) and v is the velocity of fluid. Now, to include flow inside the Tsallis distribution, we replace $E \rightarrow p^\mu u_\mu$ assuming temperature to be scalar. The dot product then becomes,

$$p^\mu u_\mu = \gamma m_T \cosh(y - \zeta) - \gamma v p_T \cos(\phi - \alpha) \quad (71)$$

Now putting Eq. (71) in Eq. (18) up to $\mathcal{O}(q-1)$ and integrating over ϕ and ζ we get,

$$\begin{aligned} \frac{1}{p_T} \frac{dN}{dp_T dy} &= \frac{gV}{(2\pi)^2} \\ & \left\{ 2T[rI_0(s)K_1(r) - sI_1(s)K_0(r)] \right. \\ & - (q-1)Tr^2I_0(s)[K_0(r) + K_2(r)] \\ & + 4(q-1)TrsI_1(s)K_1(r) \\ & - (q-1)Ts^2K_0(r)[I_0(s) + I_2(s)] \\ & + \frac{(q-1)}{4}Tr^3I_0(s)[K_3(r) + 3K_1(r)] \\ & - \frac{3(q-1)}{2}Tr^2s[K_2(r) + K_0(r)]I_1(s) \\ & + \frac{3(q-1)}{2}Ts^2r[I_0(s) + I_2(s)]K_1(r) \\ & \left. - \frac{(q-1)}{4}Ts^3[I_3(s) + 3I_1(s)]K_0(r) \right\} \end{aligned} \quad (72)$$

where

$$r \equiv \frac{\gamma m_T}{T} \quad (73)$$

$$s \equiv \frac{\gamma v p_T}{T} \quad (74)$$

$I_n(s)$ is the modified Bessel function of first kind.

References

1. C. Tsallis, *J. Statist. Phys.* **52** (1988) 479.
2. B. I. Abelev et al. (STAR collaboration), *Phys. Rev. C* **75** (2007) 064901.
3. A. Adare et al. (PHENIX collaboration), *Phys. Rev. D* **83** (2011) 052004.
4. A. Adare et al. (PHENIX collaboration), *Phys. Rev. C* **83** (2011) 064903.
5. K. Aamodt, et al. (ALICE collaboration), *Phys. Lett. B* **693** (2010) 53.
6. K. Aamodt, et al. (ALICE collaboration), *Eur. Phys. J C* **71** (2011) 1655.
7. V. Khachatryan, et al. (CMS collaboration), *J. of High Eng. Phys.* **02** (2010) 041;
8. V. Khachatryan, et al. (CMS collaboration), *Phys. Rev. Lett.* **105** (2010) 022002.
9. G. Aad, et al. (ATLAS collaboration), *New J. Phys.* **13** (2011) 053033.
10. B. Abelev, et al. (ALICE collaboration), *Phys. Rev. Letts.* **109** (2012) 252301.
11. I. Bediaga, E.M.F. Curado, J.M. de Miranda, *Physica A* **286** (2000) 156.
12. G. Wilk and Z. Włodarczyk, *Acta Phys. Polon. B* **46** (2015) 1103.
13. K. Ürmössy, G.G. Barnaföldi, T.S. Biró, *Phys. Lett. B* **701** (2011) 111.
14. K. Ürmössy, G.G. Barnaföldi, T.S. Biró, *Phys. Lett. B* **718** (2012) 125.
15. P. K. Khandai, P. Sett, P. Shukla, V. Singh, *Int. Jour. Mod. Phys. A* **28** (2013) 1350066.
16. B.-C. Li, Y.-Z. Wang and F.-H. Liu, *Phys. Lett. B* **725** (2013) 352.
17. L. Marques, J. Cleymans and A. Deppman *Phys. Rev. D* **91** (2015) 054025.
18. J. Cleymans and D. Worku, *J. Phys. G* **39** (2012) 025006.
19. J. Cleymans and D. Worku, *Eur. Phys. Jour. A* **48** (2012) 160.
20. J. Cleymans, G.I. Lykasov, A.S. Parvan, A.S. Sorin, D. Worku, *Phys. Lett. B* **723** (2013) 351.
21. M.D. Azmi and J. Cleymans, *J. Phys. G* **41** (2014) 065001.
22. Z. Tang, Y. Xu, L. Ruan, G. van Buren, F. Wang, and Z. Xu, *Phys. Rev. C* **79** (2009) 051901(R).
23. Ze-Bo Tang, Li Yi, Ji-Juan Ruan, Ming Shao, Cheng Li, *Chin. Phys. Lett.* **30** (2013) 031201.
24. T.S. Biró, G. Pürscell, K. Ürmössy, *Eur. Phys. J. A* **40** (2009) 325.
25. K. Ürmössy, T.S. Biró *J. Phys. G* **36** (2009) 064044.
26. M. Rybczyński, Z. Włodarczyk, *Eur. Phys. J. C* **74** (2014) 2785.
27. C. Beck, *Physica A* **286** (2000) 164.
28. T. Osada G. Wilk, *Phys. Rev. C* **77** (2009) 044903.
29. W.M. Alberico, A. Lavagno, and P. Quarati, *Nucl. Phys. A* **680** (2001) 94c.
30. J. Cleymans, *EPJ Web Conf.* **70** (2014) 00009.
31. S. Asgarani, B. Mirza, *Physica A* **37** (2007) 513.
32. P. K. Khandai, P. Sett, P. Shukla and V. Singh, *J. Phys. G: Nucl. Part. Phys.* **41** (2014) 025105.
33. B. De, *Eur. Phys. J A* **50** (2014) 138.
34. K. Ürmössy and T.S. Biró, *Phys. Lett. B* **689** (2010) 14.
35. D. Thakur, S. Tripathy, P. Garg, R. Sahoo and J. Cleymans, arXiv:1601.05223.
36. G. Wilk and Z. Włodarczyk, *Phys. Rev. C* **79** (2009) 054903.
37. G. Wilk and Z. Włodarczyk, *Eur. Phys. Jour. A* **40** (2009)299.
38. M. Shao, L. Yi, Z. Tang, H. Chen, C. Li and Z. Xu, *J. Phys. G* **37** (2010) 085104.
39. B. De, S. Bhattacharyya, G. Sau and S. K. Biswas, *Int. Jour. Mod. Phys. E* **16** (2007) 1687.
40. R. Witt, arXiv:nucl-ex/0403021
41. H. Hamagaki in *Perspectives of Heavy-Ion Physics* (eds. K. Yoshida, S. Kubono, I. Tanihata and C. Signorini), World Scientific Publishing Co. Pte. Ltd. Singapore 596224 (2002)
42. M. Biyajima, T. Mizoguchi, N. Nakajima, N. Suzuki, G. Wilk, *Eur. Phys. J. C* **48** (2006) 597.
43. T.S. Biró, G. Barnaföldi, P. Ván, *Physica A* **417** (2015) 215.
44. T.S. Biró, P. Ván, G. Barnaföldi, K. Ürmössy, *Entropy* **16** (2014) 6497.
45. M. Abramowitz and I.A. Stegun, *Handbook of Mathematical Functions*, National Bureau of Standards, 1972.